ENVIRONMENTAL SAMPLING WITH MULTISCALE SENSING

Xiangming Kong, Richard Pon, William Kaiser, and Gregory Pottie[*]

University of California at Los Angeles
Electrical Engineering Dept.
Los Angeles, CA 90095

ABSTRACT

Environment reconstruction through sampling is a difficult task and usually requires a large amount of resources. In this paper, a sampling technique is presented that approaches exhaustive sampling performance with only sparse samples. The goal is achieved by combining information from sensors of different types and resolutions. Image processing techniques are employed to extract global information. This information is passed on to the local sensors to optimize the number and locations of low-level sampling points. The sampled values are then applied back to the image to reconstruct the whole field. The technique is tested in the lab setup and shown to achieve a better result than traditional sampling methods.

1. INTRODUCTION

Recent advances in sensing technology have made distributed sensors an important tool in environmental monitoring. Heterogeneous fields attract more attention because they are more often encountered in the real world. Results [1][2][3] show that reconstruction of a field with a moderate number of discontinuities requires a large number of samples to achieve reasonable accuracy. Sensors incorporating limited mobility proposed by [4] enable adaptive sampling techniques [5][6]. This method reduced the amount of resources. But when the field shows fast temporal variation in addition to spatial heterogeneity, the performance of adaptive sampling can degrade significantly. Hence, better sampling techniques are needed for such fields.

Many environmental phenomena can be sampled by different types of sensors. For example, thermometers and infrared imagers can both measure temperature. Generally, different types of sensors also provide different sampling range and resolution. We developed a sampling technique that combines the measurements from different sensor modes, which will be referred to as multiscale sampling. Our hypothesis is that a combination of sparsely allocated sensors of different modes will yield the performance of exhaustive sampling.

We focus on the application of sampling the incident sunlight intensity under a forest canopy. The reasons are two-fold. First, light intensity is very important in biology for the study of photosynthesis [7][8]. Second, the field of incident sunlight intensity under a canopy demonstrates a very high spatiotemporal frequency. Fig. 1 shows the shadow made by a tree in an area of about 100cm $\times$ 80cm and its corresponding spatial distribution of light intensity. Around noon, the shade generated by a branch 3 meters above ground moves half a meter away from its original position within half an hour. This shows the fast temporal variation of the field. If sensors only collect local data, as they do in previous works [1][3], many sensors will be required to achieve high reconstruction accuracy.

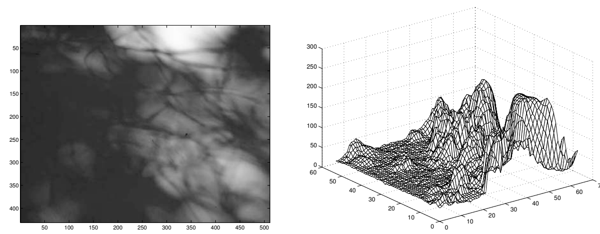

(a) Canopy shadow (b) Spatial distribution

Fig. 1. Spatial distribution of light intensity under canopy.

In [9], two different modes of data are obtained to estimate the snow water distribution. But the results from the two different scales are only compared. No fusion is performed to improve the results. Multiscale estimation and data fusion for the random field has been studied in [10] and used in geoscience applications [11][12]. These studies rely on some established model to perform Kalman filtering and data fusion. Though there are models for the distribution of sunflecks [13], statistical models for the distribution of sunlight intensity under a canopy are still under study. Hence, we developed a direct data fusion algorithm to combine measurements from different resolutions and modes.

2. MULTISCALE SENSING

Based on the characteristics of the field we studied, we selected cameras and Photosynthetic Active Radiation (PAR) sensors to provide two scales of observations [14]. Images from an overhead camera present global scale information. An actuated mobile PAR sensor collects local information. The camera has the advantage of fast sampling. However, it can only measure the reflected light intensity, affected by the ground reflectivity. Generally the reflected light intensity has a nonlinear relationship with the incident intensity. Additionally, the camera's characteristic curve of recorded light intensity vs. receiving light intensity is nonlinear. On the other hand, the PAR sensors can measure the incident light intensity more accurately, but the range of the areas they measure is limited and the mobile actuator has a slow movement rate. Our approach is to combine their measurements to overcome their respective shortcomings.

2.1. Field Model

The maximum light intensity appears in the area the sun illuminates directly, which we will refer to as sunflecks. The minimum light intensity appears in the area of deep shade. We will refer to such

[*]This material is based upon work supported by the National Science Foundation (NSF) under Grant No. ANI-00331481 and NSF graduate research fellowship. Any opinions, findings, and conclusions or recommendations expressed in this material are those of the author(s) and do not necessarily reflect the views of the National Science Foundation.

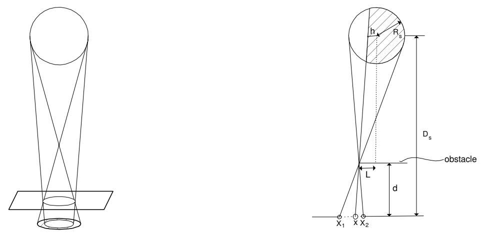

Fig. 2. Penumbral effect. (a)Basic penumbral geometry. (b)Two dimensional view of enlarged penumbra

areas as shadows. Based on the image from the camera, we partition the whole field into sunflecks, shadows and transition area.

The formation of the transition area is mainly due to the optical principle that when light originating from a non-point source passes through a circular aperture, the image it generates is composed of a bright center portion circumscribed by a shadow edge. This effect is known in biology as the penumbral effect [13] and is illustrated in Fig. 2 a). Based on the geometry of the sun, the light intensity at a point x in the transition area is (assuming the maximum intensity is 1. See Fig. 2 b)):

$$I_x = 1 + \frac{u\sqrt{1-u^2} - cos^{-1}u}{\pi} \tag{1}$$

where $u = h/R_s$

$$h = \frac{(x - \frac{x_2+x_1}{2})(D_s - d) + \frac{R_s^2}{(D_s-d)^2-R_s^2}Ld}{\sqrt{\frac{(x_2-x_1)^2}{4}\frac{(D_s-d)^2}{R_s^2} + \frac{(2x-x_2-x_1)Ld(D_s-d)-d^2R_s^2}{(D_s-d)^2-R_s^2}}}$$

and the penumbra size is:

$$x_2 - x_1 = 2dR_s\frac{\sqrt{(D_s-d)^2-(L^2-R_s^2)}}{(D_s-d)^2-R_s^2} \tag{2}$$

D_s is the distance from the sun to the earth and R_s is the radius of the sun.

The equation above is applicable when there is only one large gap. When the gap is smaller than a certain size, the intensity in the center will not reach maximum intensity. If there are multiple gaps that are close to each other, the transition area generated by each gap may overlap. Hence, we further classify the transition area into three categories: *a*) full penumbra; *b*) partial penumbra due to a small gap; *c*) partial penumbra due to multiple gaps. Fig. 3 illustrates these three scenarios and their corresponding intensity curves.

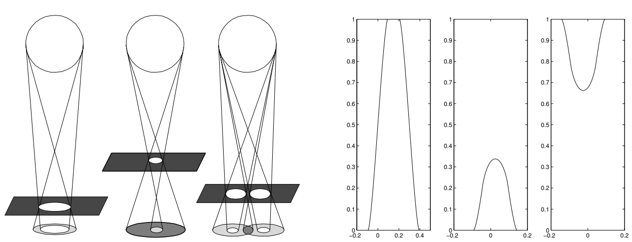

Fig. 3. Penubra classification and their corresponding intensity curve I_x: 1) full penumbra; 2) partial penumbra due to small gap; 3) partial penumbra due to multiple gaps.

3. RECONSTRUCTION ALGORITHMS

The light intensity field keeps changing and can be treated as a random process in time. So it is meaningless to reconstruct only a snapshot of the field. Instead, we assume the field is static for a short time interval and obtain the mean field over the time window.

We divide time into epochs. At the beginning of each epoch, several images are taken to obtain the mean reflected intensity. An image processing procedure is performed on the mean image to select sampling points. Then the mobile PAR sensor moves to the points picked out from the image to get the measurement of incident light intensity. At this stage, we assume that the epoch is long enough so that all the required data can be collected within the epoch. Hence the mobile sensor just moves sequentially to each point without special planning. The field is reconstructed by combining the information from the mean image and the samples. The outline of the procedure is given below.

Field Reconstruction

1. Obtain mean image at the beginning of a time epoch.
2. Partition the image into homogeneous subfields.
3. Check the smoothness of each subfield.
4. Sample smooth fields and reconstruct through interpolation.
5. Locate and reconstruct penumbra.
6. Reconstruct the subfields left over.

3.1. Field Partition

The heterogenous field can be partitioned into smaller homogeneous subfields. Each subfield requires a different number of samples to reach a certain reconstruction fidelity depending on its spatial frequency. By allocating less samples to the smoother subfields, we can reduce the total number of samples significantly.

The camera provides the information needed to perform the field partition. When the ground reflectivity is uniform, the reflective light intensity falls into the same category as the incident light intensity, i.e, the sunflecks, shadows and transition areas in the image correspond to the sunflecks, shadows and transition areas in the incident light field. These different intensity categories create different features in the image. When an object on the ground changes the ground reflectivity, it also adds different features such as different colors in the image. Therefore, we can segment the image based on the features in the image to fulfill the field partition process.

When segmenting the image, no previous knowledge is assumed about features in the image. Instead, the features are recognized from the statistical distribution of pixels' values. Pixels with similar features form a cluster in the pixel value distribution. Peaks in the distribution (i.e., the cluster center) are located through the mean shift algorithm [15]. The algorithm presented in [16] is applied to improve the processing speed. Pixels having strong features are allocated to feature clusters. Pixels having weak features are grouped together and are treated as a special cluster.

Once all the pixels are allocated to certain feature clusters, all the connected pixels in the same cluster are recognized as an object. In this way, the image is segmented into objects. Objects smaller than a certain size are treated as noise and merged into larger objects. Sunflecks and shadows usually exhibit strong features in the image while transition areas exhibit weak features. Hence, after the image segmentation step, the field is partitioned into smaller homogeneous subfields in the three categories.

3.2. Field Reconstruction

Even though the camera cannot measure the incident light intensity accurately, it can provide a good indication on the smoothness of each subfield. The camera response curve is linear in the middle intensity range and sublinear in the low and high intensity range. In the image segmentation step, subfields in different intensity ranges are separated since they show different features. A smooth subfield in the middle intensity range in the image indicates that the incident light subfield is also smooth. For the subfield in the low intensity range, pixel intensity value in the image is calibrated based on the camera response curve. Then the variance of pixel intensity is computed to check the smoothness of the subfield. In these two types of subfields, if the variance of the pixel intensity value is smaller than a threshold, samples are taken randomly by PAR sensors within each subfield without further processing. The number of samples required is determined by the variance and the subfield size.

The photosynthesis process saturates at a certain light intensity level (depending on the plants, the saturation light intensity is different). Experimental results show that light intensity in sunflecks is above the saturation intensity most of the time during the day. Subfields in the high intensity range in the image result from two different scenes: *a*) a sunfleck; *b*) an object with strong reflectivity such as glass. Hence, one sample is taken first by a PAR sensor in the subfield. If it is above the saturation light intensity, the subfield is claimed to be a sunfleck and the whole subfield is assumed to be above the saturation intensity. No further samples are taken in the subfield and the intensity value of the sample is used as the intensity value of all pixels. If the sample intensity value is below the saturation intensity, the same reconstruction procedure as the subfield in the low intensity range is applied to this subfield. Since the interpolation method is not the focus of our current research, linear interpolation is applied for simplicity. Better interpolation technique can be employed later to further improve the results.

A portion of the remaining subfields is penumbra. The number of samples required can be reduced substantially by applying the penumbra model developed in section 2. Since penumbra form from partial obscurity of the sun, they mainly exist around the sunflecks. So we focus our attention on subfields surrounding sunflecks. As shown in equation (2), the penumbra size only depends on the sun angle and the distance between the gap generating the penumbra and ground. When the sun angle is fixed, the size of the penumbra generated by a gap is also fixed. Pixels in the penumbra with the same distance to the boundary of a sunfleck have the same intensity. Intensity in full penumbra is highly linear. So linear interpolation is applied after one sample at the boundary of the penumbra and one sample at the boundary of the sunfleck are taken. By sampling a whole line connecting the boundary of the sunfleck and the boundary of the penumbra, light intensity in the partial penumbra can be obtained. The procedure is illustrated in the following pseudocode.

Pseudocode description of nonsmooth field reconstruction

```
for eachnonsmooth subfield {
    find neighboring sunflecks
    for each neighbor sunfleck S {
        Dilate S until a shadow is encountered or the whole
            subfield is included. Denote the portion of the
            subfield included by F
        Record distance of each pixel in F to boundary of S
        Subdivide F into areas neighboring to same patches*
        for each area A {
            if it is full penumbra
                {Sample at boundaries and linearly interpolate}
            else {Sample along a radial line** in F}
            Reconstruct A
        }
    }
}
Interpolate the reconstructed pixels to fill up the whole field
```

*Patches refer to the smooth subfields having been reconstructed.
**A radial line is a line radiating from the center of the sunspeck.

4. EXPERIMENTAL RESULTS

Due to the difficulties in collecting ground truth data in the real field, a simulated field in a lab is setup to validate our hypothesis. A lamp functioning as the sun projects light on a screen. Between the lamp and the screen, obstacles are placed to cast shadows. The screen has uniform reflectivity. To simulate the nonuniform reflectivity of the ground, the screen is decorated with objects of various materials. At this stage, we assume that the camera domain and the PAR sensor domain are perfectly aligned so that each pixel in the image corresponds to a point in the PAR sensor domain. An image of the screen without decoration on it is also taken. The image is then corrected against the camera response curve. Pixel intensity values in such an image are proportional to the incident light intensity and can be used as ground truth.

Fig. 4(a) shows light field in the lab setup. The corresponding partitioned field is shown in Fig. 4(b). Each object is given a different label and represented in pseudocolor. From this figure, it is obvious that most of the sunflecks, shadows and penumbra have been separated. Notice that penumbra surrounding sunflecks are partitioned as different objects. Fig. 4(c) demonstrates the reconstructed field. Comparing with the ground truth shown in Fig. 4(d), we can see that most of the sunflecks and shadows are faithfully reconstructed. Because of the large pixel value range, reconstruction results for the transition areas cannot be clearly observed in this figure. To reduce the pixel value range, ground truth is subtracted from the reconstructed field and the error image is presented in Fig. 4(e). It can be seen that most of the transition area has a small reconstruction error (darker color corresponds to smaller error). For comparison, the intensity image of the Fig. 4(a) is also displayed in Fig. 4(f). Apparently, if we use this image to measure the light field, a large measurement error can be expected. Finally, the number of samples and reconstruction mean square error (MSE) of different sampling methods are presented in Table 1. Compared to other methods, a better reconstruction result with fewer samples is achieved by the multiscale technique we proposed here.

Table 1. Comparison with Other Sampling Methods

	Number of Samples	MSE
Multiscale	239	0.0535
Rahimi[6]	274	0.0883
Willett*[17]	2432	0.0539
Raster	413	0.0592

*One advantage of [17] is combating noise. So noise with $\sigma^2 = 0.21$ is added. Since the method is an image processing technique, it requires a large number of samples to gain knowledge of the field.

The reconstruction result for a real scene is presented in Fig.5. 365 samples are used with the final reconstruction MSE 0.0655. Due to the lack of the ground truth, we used the intensity image of the scene as the ground truth and take samples from it. Hence, the MSE should be better than using real ground truth. But the resulting image reveals that most of the areas, especially the sunflecks, are reconstructed correctly in such a complex scene.

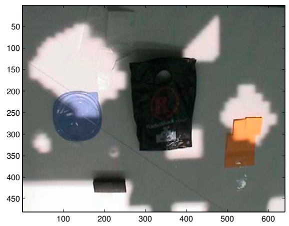

(a) Image of the light field

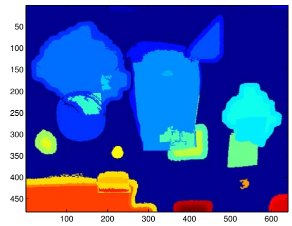

(b) Partitioned light field

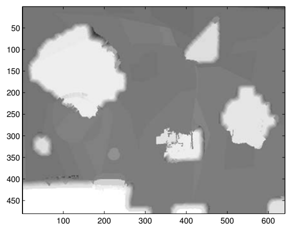

(c) Reconstructed light field

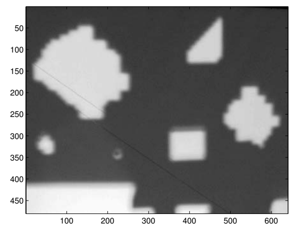

(d) Ground truth image

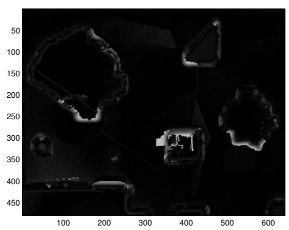

(e) Reconstruction error

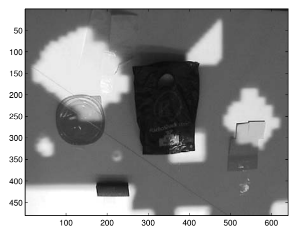

(f) Intensity in decorated image

Fig. 4. Test result for nonuniform ground reflectivity.

5. CONCLUSIONS AND FUTURE WORKS

In this paper, we proposed a new method to sample the field with high spatial frequency through different types of sensors. Results show that by combining measurements from different scales and modes, we can reduce the number of samples significantly without compromise in the reconstruction accuracy.

In the incident light intensity reconstruction problem, since the movement, position and intensity of the sun can be easily determined, work is going on to track the location and size of the sunflecks and shadows. The number of samples are expected to be further reduced by predicting the intensity in the sunflecks and shadows. In the future, we will plan the mobile PAR sensor's sampling route and prioritize the samples that reduce the MSE most to reconstruct the fast changing heterogeneous field. Combination with better interpolation methods (both spatial and temporal) and more general use of better models are other tracks for future research.

(a) Image of the light field

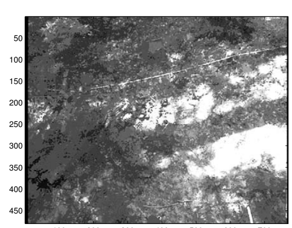

(b) Reconstructed light field

Fig. 5. Test result for a real scene

6. REFERENCES

[1] R. Nowak, U. Mitra, and R. Willett, "Estimating inhomogeneous fields using wireless sensor networks," *IEEE Journal on Selected Areas in Commu.*, vol. 22, pp. 999–1006, 2004.

[2] David L. Donoho, "Wedgelets: Nearly minimax estimation of edges," *The Annals of Statistics*, vol. 27, pp. 859–897, 1999.

[3] A. Kumar, P. Ishwar, and K. Ramchandran, "On distributed sampling of smooth non-bandlimited fields," in *IPSN*, 2004, pp. 89–98.

[4] W. Kaiser, G. Pottie, M. Srivastava, G. Sukhatme, J. Villasenor, and D. Estrin, "Networked infomechanical systems (nims) for ambient intelligence," *CENS Tech Report*, , no. #31, 2003.

[5] M. Rahimi, R. Pon, W. Kaiser, G. Sukhatme, D. Estrin, and M. Srivastava, "Adaptive sampling for environmental robotics," in *ICRA*, 2004, pp. 3537–3544.

[6] M. Rahimi, M. Hansen, W. J. Kaiser, G. S. Sukhatme, and D. Estrin, "Adaptive sampling for environmental field estimation using robotic sensors," in *IEEE/RSJ Int. Conf. on Intelligent Robots and Systems*, 2005.

[7] M. M. Caldwell and R. W. Pearcy, *Exploitation of Environmental Heterogeneity by Plants: Ecophysiological Processes Above- and Belowground*, chapter 2, pp. 21–71, Academic Press, 1994.

[8] R. W. Percy, "Sunflecks and photosynthesis in plant canopies," *Annu. Rev. Plant Physiol. Plant Mol. Biol.*, vol. 41, pp. 421–453, 1990.

[9] C. Derksen, A. E. Walker, B. E. Goodison, and J. W. Strapp, "Integrating in situ and multiscale passive microwave data for estimation of subgrid scale snow water equivalent distribution and variability," *IEEE Trans. on Geoscience and Remote Sensing*, vol. 43, pp. 960–972, 2005.

[10] K. C. Chou, A. S. Willsky, and A. Benveniste, "Multiscale recursive estimation, data fusion, and regularization," *IEEE Trans. on Automatic Control*, vol. 39, pp. 464–478, 1994.

[11] K. C. Slatton, M. M. Crawford, and B. L. Evans, "Fusing interferometric radar and lasor altimeter data to estimate surface topography and vegetation heights," *IEEE Trans. on Geoscience and Remote Sensing*, vol. 39, pp. 2470–2482, 2001.

[12] P. W. Fieguth, W. C. Karl, A. S. Willsky, and C. Wunsch, "Multiresolution optimal interpolation and statistical analysis of topex/poseidon satellite altimetry," *IEEE Trans. on Geoscience and Remote Sensing*, vol. 33, pp. 280–292, 1995.

[13] E. E. Miller and J. M. Norman, "A sunfleck theory for plant canopies. part ii. penumbra effect: Intensity distributions along sunfleck segments," *Agronomy Journal*, vol. 63, pp. 739–743, 1971.

[14] W. K. Smith, A. K. Knapp, and W. A. Reiners, *Radiation and Light Measurements*, chapter 6, pp. 97–116, Chapman and Hall, London, U.K., 1989.

[15] Y. Cheng, "Mean shift, mode seeking, and clustering," *IEEE Trans. Pattern Anal. Machine Intell.*, vol. 17, pp. 790–799, 1995.

[16] D. Comaniciu and P. Meer, "Robust analysis of feature spaces: Color image segmentation," in *IEEE Proc. Computer Vision and Pattern Recognition*, 1997, pp. 750–755.

[17] R. Willett, A. Martin, and R. Nowak, "Backcaster: Adaptive sampling for sensor networks," in *IPSN*, 2004, pp. 124–133.